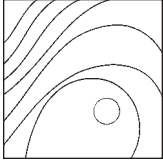


Osseoincorporation of Porous Tantalum Trabecular-Structured Metal: A Histologic and Histomorphometric Study in Humans



Celia Clemente de Arriba, MD¹
 Miguel Angel Alobera Gracia, BDS, MSD²
 Paulo G. Coelho, DDS, PhD³/Rodrigo Neiva, DDS, MS⁴
 Dennis P. Tarnow, DDS⁵/Mariano del Canto Pingarron, BDS²
 Soledad Aguado-Henche, MD¹

Porous tantalum trabecular-structured metal (PTTM) has been applied to titanium orthopedic and dental implants. This study evaluated the healing pattern of bone growth into experimental PTTM cylinders (N = 24; 3.0 × 5.0 mm) implanted in the partially edentulous jaws of 23 healthy volunteers divided into four groups. Six PTTM cylinders per group were explanted, prepared, and analyzed histologically/metrically after 2, 3, 6, and 12 weeks of submerged healing. PTTM implant osseoincorporation resulted from the formation of an osteogenic tissue network that over the course of 12 weeks resulted in vascular bone volume levels in PTTM that are comparable to clinically observed mean trabecular volumes in edentulous posterior jaws. Int J Periodontics Restorative Dent 2018 (7 pages). doi: 10.11607/prd.3004

The ability to achieve and maintain osseointegration has resulted in a high degree of predictability for dental implants, often with long-term survival rates well above 90%.¹⁻³ Although the risk of implant failure remains relatively low, its occurrence can be detrimental for the patient and can pose significant challenges.

Implant survival rates are directly related to the quality of the bone-to-implant interface.⁴ Numerous studies in the dental literature have reported that implant and hard tissue osseointegration is positively affected by altering the characteristics of the machined (turned) implant surface.⁴ For that purpose, a variety of ablative (grit-blasting, laser- or acid-etching, anodization), additive (plasma spraying, electrophoretic deposition, sputter deposition, sol gel coating, pulsed laser deposition, biomimetic precipitation),⁴ and combination surface modifications^{5,6} have been introduced to increase the percentage of bone interaction with the implant and ultimately enhance the quality of host-to-implant integration. Among these modifications, porous surface coatings have been designed to enhance implant fixation by permitting bone ingrowth into small bone healing chambers, or pores, formed by the implant geometric characteristics.⁵ These pores may undergo a different bone healing process

¹Full Professor of Human Anatomy and Embryology, Department of Surgery, Anatomy and Social Sciences, University of Alcalá de Henares, Madrid, Spain.

²Codirector of Oral Biology, Implantology and Periodontology, University of León, Campus de Vegazana S/N, León, Spain.

³Associate Professor of Biomaterials and Biomimetics, New York University, New York, New York, USA.

⁴Clinical Associate Professor of Periodontology, University of Florida, Gainesville, Florida, USA.

⁵Clinical Professor of Periodontology and Director of Implant Education, Columbia School of Dental Medicine, and Private Practice in Periodontology and Implant Dentistry, New York, New York, USA.

Correspondence to: Dr Paulo G. Coelho, Department of Biomaterials and Biomimetics, New York University, 433 1st Ave, Room 10010, New York, NY 10010, USA.
 Email: pgcoelho@nyu.edu

©2018 by Quintessence Publishing Co Inc.

where rapid bone formation occurs through an intramembranous-like healing pathway. However, the volume and quality of achievable bone ingrowth into porous surface coatings is limited by the number and size of the pores. For example, while pores of 100 μm allow bone ingrowth, larger pores of 150 μm are needed for osteon formation, and pores $> 300 \mu\text{m}$ are required for angiogenesis inside the material. Nonetheless, surfaces with various pore sizes have been regarded as having adequate continuity for bone ingrowth and maturation.⁵

To address the limited amount of bone ingrowth achievable with porous surface coatings, orthopedic researchers developed highly porous (~80%), tantalum trabecular-structured metal (PTTM) (Trabecular Metal Material, Zimmer Biomet), a biomaterial that forms a three-dimensional network of interconnected pores in highly regular sizes (~430 μm) and shapes designed for bone and blood vessel ingrowth. The physicochemical characterization of PTTM has been reported in detail elsewhere, and its mechanical properties more closely approximate that of natural bone (6.8 to 17 GPa) than solid titanium (106 to 115 GPa) and other surgical metals (210 to 230 GPa).⁷⁻¹⁰

PTTM and other methods have been applied to orthopedic titanium hip, knee, and spine implants since 1997,¹¹⁻¹³ and more recently to titanium dental implants.¹⁴⁻¹⁶ For instance, implants that allow healing chamber formation (defined as void spaces between the surgical instrumentation outer diameter and the implant

bulk component, where a blood clot will be present immediately after implantation) after placement have been known for rapid bone formation¹⁷⁻²⁰ and the development of haversian-like structures²¹⁻²⁴ over the implantation time. Under the same prerogative, the PTTM trabecular structure and crystallographic surface texture created by the CVD process have been reported by the manufacturer to increase the percentage of surface area of PTTM dental implants by 52.7% to 81.8%, depending on implant diameter. Although the biocompatibility and efficacy of the PTTM dental implant design has been documented through animal and limited size human clinical studies,^{25,26} the temporal bone ingrowth inside PTTM has not been well documented in dental clinical models during early implantation times. The present study histologically and histomorphometrically evaluated PTTM cylinders placed in human jaws.

Materials and Methods

This study conformed to the ethical principles for medical research involving human subjects specified in the World Medical Association's Declaration of Helsinki (amended October 2013). Subjects' rights were protected by the University of Léon institutional review board (approval letter July 20, 2011), and written informed consent was granted by each subject.

Systemically healthy, partially edentulous volunteers were scheduled for implant placement in one

or both jaws. Study candidates were required to have adequate residual bone to accommodate placement and explantation of a 3.0-mm-diameter, 5.0-mm-long PTTM cylinder. The study design allowed up to four nonadjacent PTTM cylinders to be placed in a single subject. After explantation, subjects were provided with a dental implant and/or bone graft, as determined by the clinician based on patient needs. Subjects were clinically and radiographically evaluated preoperatively using computed tomography (CT) to verify adequate ridge dimensions and the location of anatomical landmarks. Participants were randomly assigned to one of four treatment groups designated for PTTM cylinder explantation after 2, 3, 6, or 12 weeks of healing. Each treatment group interval consisted of six PTTM cylinders.

Under local anesthesia, the implantation site was surgically exposed. Osteotomies were sequentially prepared under irrigation by first using a pilot drill 2.3 mm in diameter and 6 mm long, followed by final sizing with an internally irrigated spade drill 2.8 mm in diameter and 6 mm long. Implantation sites were located between or distal to preexisting dental implants. A sterile cylinder was pressed into the osteotomy until it was fully seated. Because healing would be submucosal and the final osteotomies were 2.8 mm in diameter, which was 0.2 mm smaller than the PTTM cylinders, there was not major concern about cylinder micromovement in the absence of threads on the PTTM samples due to PTTM's high coefficient of friction

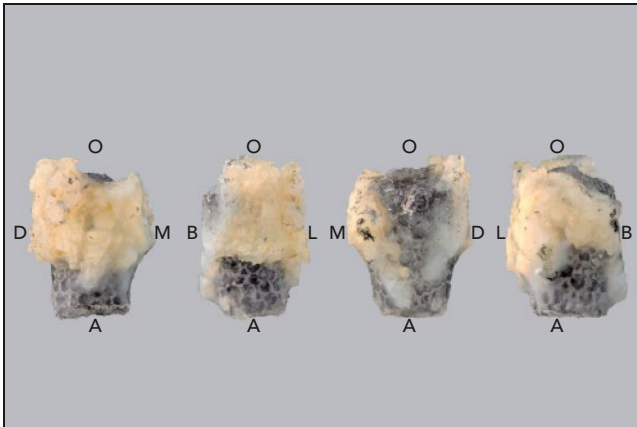


Fig 1 Explanted cylinders were marked to indicate their orientation at placement: apical (A), coronal (O), mesial (M), distal (D), buccal (B), lingual (L). Four possible orientations of one explanted cylinder are shown (left to right): buccal, mesial, lingual, distal.

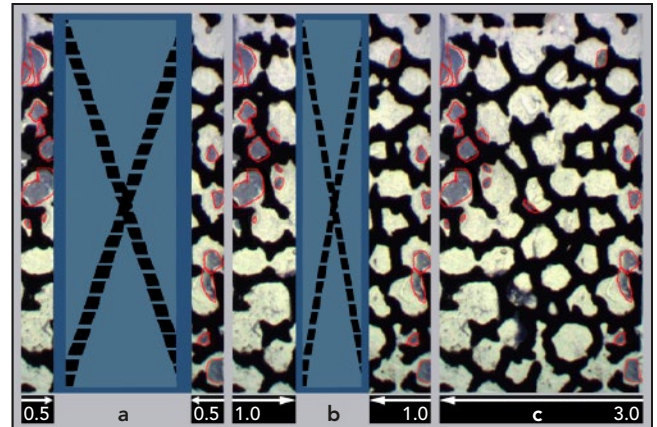


Fig 2 Percentage of area density (%Aa) was assessed in three different regions, as measured in mm from the outside peripheral surface of the PTTM cylinder: (a) partial sample to a depth of 0.5 mm (0.5 mm wide \times 5.0 mm long); (b) partial sample to a depth of 1 mm (1.0 mm wide \times 5 mm long); and (c) the entire sample (3.0 mm wide \times 5.0 mm long).

against bone.²⁶ Soft tissues were approximated and sutured for primary closure. Subjects were reappointed for cylinder explantation according to their previously assigned treatment group. A periapical radiograph of the PTTM cylinder was taken immediately prior to explanation (5.0-mm-diameter trephine). Additional intermediate periapical radiographs were also taken at 4 weeks for subjects in the 6-week explantation group, and at 4 and 8 weeks for patients in the 12-week explantation group. After removal, the PTTM cylinder and surrounding bone tissue were physically marked to distinguish the sample's apical, coronal, buccal, and lingual orientations at placement (Fig 1). The explanted cylinder was then placed in 10% buffered formaldehyde and sent to the laboratory for histologic processing and analysis.

Histologic Analysis

The 3.0-mm-diameter nondecalcified explanted implants were embedded in polymethylmethacrylate and cut parallel to the apicocoronal long axis of the cylinder. Slides were stained for histologic analysis. The percentage of bone area density (%Aa) was assessed in three different regions, as measured from the outside peripheral surface of the PTTM cylinder: (1) partial sample to a depth of 0.5 mm (0.5 \times 5.0 mm); (2) partial sample to a depth of 1.0 mm (1.0 \times 5.0 mm); and (3) the entire sample (3.0 \times 5.0 mm) (Fig 2). The reference area corresponded to the entire area occupied by the trabeculae of the cylinders. The area of interest for each analysis was the designated portion of the cylinders except for the areas occupied by the PTTM. To quantify the bone found

in the PTTM pores, the total tissue area density (total Aa) was calculated based on the percentage of bone area fraction occupancy within the total trabecular area of interest. Areas of bone inside the total pore area were identified and traced manually on the computer image to facilitate quantification of bone ingrowth, as described and illustrated in Fig 2. At each of the postoperative periods of 2, 3, 6, and 12 weeks, average difference of percentage of bone ingrowth between different depths were tested by Wilcoxon signed rank test. *P* values were not adjusted for multiplicity.

Results

A total of 24 PTTM cylinders were implanted in 23 subjects (16 men, 7 women), who ranged in age from

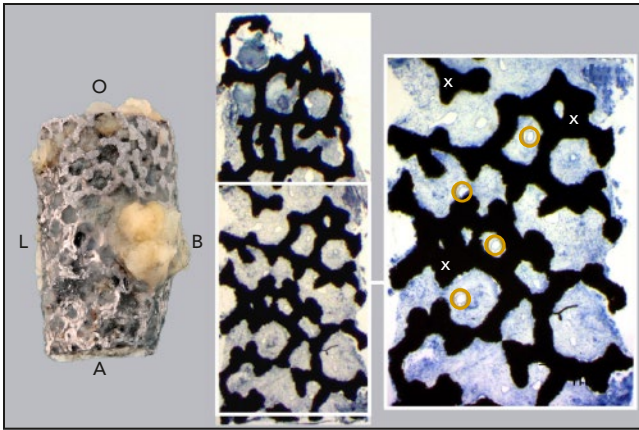


Fig 3 Week 2, distal orientation: Representative sample (left; mesial aspect) with corresponding histology section (middle); enlarged region of interest (right) shows TM (x) pores occupied by infiltration tissue and newly formed blood cells (circles) (staining: toluidine blue).

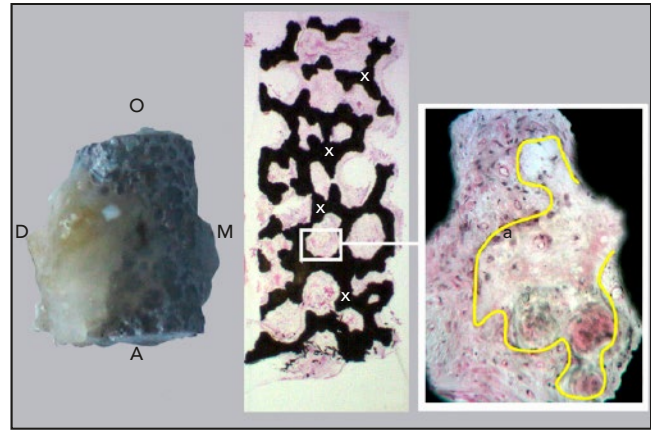


Fig 4 Week 3, buccal orientation: A front of osteoblasts (line) in an internal pore of the PTTM cylinder suggests osteogenic tissue in the process of new bone formation (staining: hematoxylin-eosin).

39 to 60 years (mean 42.13 years). At each time point of 2, 3, 6, and 12 weeks postoperative, 6 PTTM cylinders were explanted. One subject (#15) in the 6-week treatment group provided two samples: one from the maxillary left and one from the maxillary right first premolar locations. The other 22 subjects provided one sample each. By jaw, 14 PTTM cylinders (58.3%) were placed in maxillary locations and 10 (41.7%) were placed in mandibular locations. The most frequent implantation site was the second molar location ($n = 10$), followed by the first molar ($n = 4$), first premolar ($n = 4$), canine ($n = 4$), and central incisor ($n = 2$) areas. No complications were reported at any time during the study.

At 2 weeks in vivo, the pores inside the cylinders showed connective tissue infiltration with blood vessels (Fig 3). Minimal woven bone formation was observed at the PTTM walls at this time interval. Two

samples presented mild inflammatory infiltrate, and epithelial tissue of mucosal origin had invaded several peripheral pores in the cervical region. The absence of macrophages, foreign body giant cells, and significant inflammation evidenced the biocompatibility of the devices. Small bone fragments that abraded from the surface walls of the osteotomy during cylinder placement were present in the peripheral pores of some samples in mean percentages of 2.46% at a depth of 0.5 mm, 1.44% at a depth of 1 mm, and 1.34% for the whole sample (Table 1) (Fig 3). At 3 weeks, osteoblasts were observed in the connective tissue matrix in proximity with external PTTM spaces. These were located in the central pores deeper inside several of the PTTM networks and were evidence of cell migration through the osteogenic tissue (Fig 4). Infiltration of epithelial cells from the surrounding gingiva was observed at the

same level at 2 weeks in vivo. The vast majority of pores in the samples exhibited tissue infiltration with newly formed blood vessels. The mean percentage of newly formed bone is presented in Table 1.

At 6 weeks, the PTTM cylinder pores were occupied by osteogenic tissue. Larger amounts of bone were qualitatively observed relative to the 2- and 3-week samples (Fig 5, Table 1). At this time in vivo, abundant blood vessel formation was observed inside the PTTM pores. The presence of undifferentiated cells, together with bone formation activity and extensive angiogenesis, resulted in higher degrees of integration than samples retrieved at the earlier time intervals (Figs 3 and 4). Increased bone formation activity was present around and inside the PTTM pores than with samples explanted at weeks 2 and 3. At week 12, newly formed bone presenting osteoid edges lined by osteoblasts

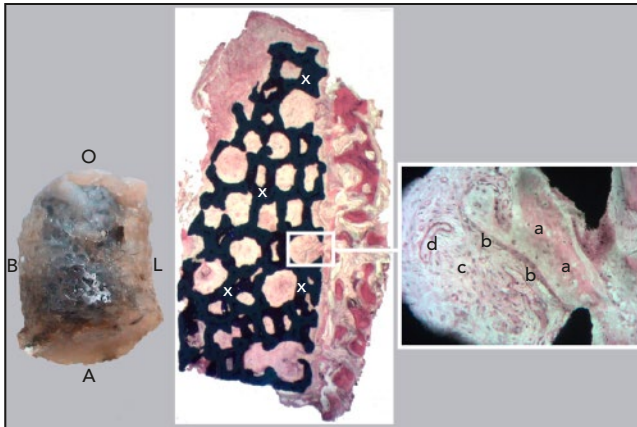


Fig 5 Week 6, distal orientation: Representative sample (left; distal aspect) with corresponding histology section (middle), peripheral pore inside the TM material (right; x) shows (a) bone tissue formation (woven bone), (b) a line of osteoblasts, (c) potentially osteogenic tissue, and (d) a longitudinally cut blood vessel (staining: hematoxylin-eosin).

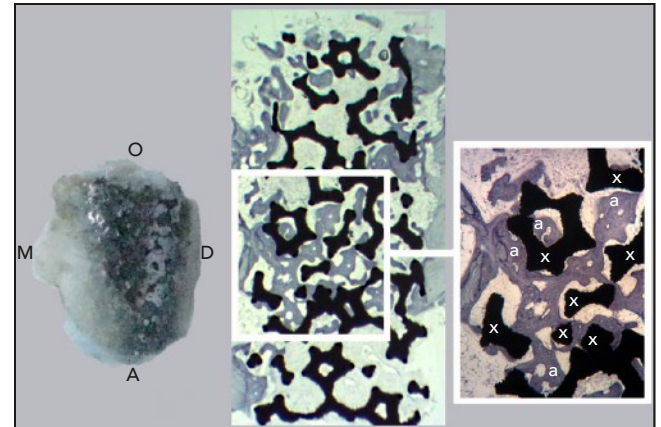


Fig 6 Week 12, lingual orientation: Representative sample (left; lingual aspect) with corresponding histology section (middle) that shows young bony trabeculae in the neoformation process with a border lined with osteoblasts penetrating the width of the cylinder. Enlarged region of interest (right) shows the young bone tissue (a) adhering to the surfaces and growing into the pores of the TM (x) material (staining: toluidine blue).

Table 1 Longitudinal Bone Ingrowth and Neoformation Inside PTTM Pores

Time interval	Depth (mm)	Samples (n)	Bone formation (%)				Comparisons of mean percentage of calcified bone vs marrow (P ^a)	
			Mean	SD	Min	Max	Differences between measurement depths	Differences between time intervals
Week 2	0.5	6	2.46 ^b	2.02	0.63	6.31		
	1	6	1.44 ^b	1.24	0.43	3.86		
	Full sample	6	1.34 ^b	0.92	0.68	3.02		
Week 3	0.5	6	2.02	2.32	0.19	6.49	.094 ^c	.174 ^d
	1	6	1.39	1.45	0.12	4.11	.94 ^e	.174 ^d
	Full sample	6	1.32	1.33	0.08	3.76	.563 ^f	.126 ^d
Week 6	0.5	6	4.75	3.87	0	10.20	.125 ^c	.008 ^g
	1	6	3.63	2.67	0	6.47	.813 ^e	.020 ^g
	Full sample	6	4.53	3.94	0	10.43	.438 ^f	.020 ^g
Week 12	0.5	6	22.74	11.91	8.35	43.04	.031 ^c	.005 ^h
	1	6	16.77	9.84	4.23	34.20	.031 ^e	.005 ^h
	Full sample	6	14.95	8.21	3.26	27.77	.31 ^f	.008 ^h

^aWilcoxon sign rank tests not adjusted for multiplicity/family-wise errors.

^bAt week 2 only, these figures represent small fragments of old bone that abraded from the surface walls of the osteotomy during placement and collected inside the peripheral pores of the TM material.

^c0.5 mm vs 1 mm.

^dWeek 3 vs week 6.

^e0.5 mm vs full cylinder.

^f1 mm vs full cylinder.

^gWeek 6 vs week 12.

^hWeek 3 vs week 12.

was observed throughout the PTTM pores (Fig 6). These were frequently in contact with the internal and ex-

ternal surfaces of the PTTM cylinders. Bone growth into the PTTM cylinders occurred mainly from the

peripheral lingual and buccal edges of the material, but no preferences were observed for either of the loca-

tions. Besides bone, blood vessels, marrow, and abundantly vascularized connective tissue were found inside the pores. A significant increase in woven bone occupancy as a function of depth was observed relative to the shorter evaluation times (Table 1).

Discussion

Titanium fiber mesh dental implants introduced in the 1970s featured a high degree of porosity, similar to PTTM.²⁷ While partial bone ingrowth into the material was documented in animals, the implants were also subject to soft tissue ingrowth and fibrous tissue encapsulation.²⁷ Such results may be attributable at least in part to the implant design. The implant lacked threads for stabilization in bone and was a one-piece device that included a transmucosal abutment post that extended into the oral cavity at the time of implant placement.²⁷ Even if the implant wasn't immediately loaded with a prosthesis, the implant post could have been indirectly loaded by tongue thrusts, cheek pressure, and impacts by food boluses during meals, which could have resulted in deleterious micro-movements by the implant with subsequent soft tissue encapsulation. In contrast, while miniature PTTM prototypes were used in the present study instead of commercially available implants, without a barrier membrane to avoid soft tissue ingrowth in PTTM, histologic sections revealed that only a few of the cylinders exhibited soft tissue ingrowth that was limited to their coronal peripheral pores and did not preclude osseointegration.

The present investigation is the first longitudinal study to histomorphometrically document progressive bone ingrowth into PTTM in human jaws. Results demonstrated that the combination of traditional bone-to-implant surface contact (through geometric interference) supplemented by an intramembranous-like bone formation in the interconnected PTTM trabecular network are in direct agreement with what has been previously characterized in the dental literature as osseoincorporation.¹⁵ While at 2 weeks the samples showed osteogenic tissue formation and filling of the PTTM spaces, at 3 weeks samples exhibited initial bone formation in the central regions of PTTM void spaces without direct contact with the biomaterial. This is likely due to the migration of bone-forming cells that initially migrated through the fibrin network developed after blood clotting in the empty spaces (healing chambers) of the PTTM.²⁸ The natural progressive osseoincorporation of the PTTM cylinders was observed from 3 to 12 weeks. At 6 and 12 weeks, newly formed bone surrounded by osteoid in intimate contact with cuboidal cells indicative of osteoblasts was evident inside and on the surfaces of the samples.

On the commercially available PTTM dental implant design, the PTTM depth ranges from approximately 0.65 to 0.76 mm, depending on the implant diameter, and the material is limited to the midsection of the implant body. For this reason, the present study evaluated the mean percentage of bone tissue formation at depths of 0.5 mm and 1.0 mm in-

side the PTTM cylinders in addition to the entire sample. The finding of approximately 23% calcified bone penetration at a depth of 0.5 mm inside the cylinders after 12 weeks of healing was not unexpected since the majority of cylinders ($n = 14/24$) were placed in posterior jaws, where mean trabecular bone volume in the first molar region has been reported to range from approximately 24% for men to approximately 18% for women in edentulous jaws.^{29,30} Similarly, sinus lifts typically have approximately 25% vital bone in histology taken from the same region after 6 to 8 months of healing.³¹ Thus, the present results show that bone regeneration throughout the PTTM network occurs to levels clinically observed prior to implant placement after 12 weeks.

Conclusions

PTTM was progressively anchored via a rapid, intramembranous-like bone healing pathway. This osseoincorporation process resulted from the formation of an osteogenic tissue network that over the course of 12 weeks resulted in vascular bone volume levels within PTTM that are comparable to clinically observed mean trabecular volumes in edentulous posterior jaws.

Acknowledgments

The authors thank Hai Bo Wen, PhD; Kim Bradbury, BS, CCRA; Na Ren, MS; Jose Puche; and Michael M. Warner, MA, for their assistance. The authors reported no conflicts of interest related to this study.

References

1. Harel N, Piek D, Livne S, Palti A, Ormianer Z. A 10-year retrospective clinical evaluation of immediately loaded tapered maxillary implants. *Int J Prosthodont* 2013;26:244–249.
2. Ormianer Z, Patel A. The use of tapered implants in the maxillae of periodontally susceptible patients: 10-year outcomes. *Int J Oral Maxillofac Implants* 2012;27:442–448.
3. Ormianer Z, Piek D, Livne S, et al. Retrospective clinical evaluation of tapered implants: 10-year follow-up of delayed and immediate placement of maxillary implants. *Implant Dent* 2012;21:350–356.
4. Goldman M, Juodzbalys G, Vilkinis V. Titanium surfaces with nanostructures influence on osteoblasts proliferation: A systematic review. *J Oral Maxillofac Res* 2014;5:e1.
5. Spector M. Historical review of porous-coated implants. *J Arthroplasty* 1987;2:163–177.
6. Vandamme K, Naert I, Vander Sloten J, Puers R, Duyck J. Effect of implant surface roughness and loading on peri-implant bone formation. *J Periodontol* 2008;79:150–157.
7. Cohen R. A porous tantalum trabecular metal: Basic science. *Am J Orthop* 2002;31:216–217.
8. Hacking SA, Bobyn JD, Toh K, Tanzer M, Krygier JJ. Fibrous tissue ingrowth and attachment to porous tantalum. *J Biomed Mater Res* 2000;52:631–638.
9. Levine B, Della Valle CJ, Jacobs JJ. Applications of porous tantalum in total hip arthroplasty. *J Am Acad Orthop Surg* 2006;14:646–655.
10. Nasser S, Poggie RA. Revision and salvage patellar arthroplasty using a porous tantalum implant. *J Arthroplasty* 2004;19:562–572.
11. Tsao AK, Roberson JR, Christie MJ, et al. Biomechanical and clinical evaluations of a porous tantalum implant for the treatment of early-stage osteonecrosis. *J Bone Joint Surg Am* 2005;87(Suppl 2):22–27.
12. Unger AS, Lewis RJ, Gruen T. Evaluation of a porous tantalum uncemented acetabular cup in revision total hip arthroplasty: Clinical and radiological results of 60 hips. *J Arthroplasty* 2005;20:1002–1009.
13. Wigfield C, Robertson J, Gill S, Nelson R. Clinical experience with porous tantalum cervical interbody implants in a prospective randomized controlled trial. *Br J Neurosurg* 2003;17:418–425.
14. Battula S, Lee JW, Wen HB, Papanicolaou S, Collins M, Romanos GE. Evaluation of different implant designs in a ligature-induced peri-implantitis model: A canine study. *Int J Oral Maxillofac Implants* 2015;30:534–545.
15. Bencharit S, Byrd WC, Altarawneh S, et al. Development and applications of porous tantalum trabecular metal-enhanced titanium dental implants. *Clin Implant Dent Relat Res* 2014;16:817–826.
16. Kim DG, Huja SS, Tee BC, et al. Bone ingrowth and initial stability of titanium and porous tantalum dental implants: A pilot canine study. *Implant Dent* 2013;22:399–405.
17. Baires-Campos FE, Jimbo R, Bonfante EA, et al. Drilling dimension effects in early stages of osseointegration and implant stability in a canine model. *Med Oral Patol Oral Cir Bucal* 2015;20:e471–e479.
18. Beutel BG, Danna NR, Granato R, et al. Implant design and its effects on osseointegration over time within cortical and trabecular bone. *J Biomed Mater Res B Appl Biomater* 2016;104:1091–1097.
19. Coelho PG, Granato R, Marin C, et al. The effect of different implant macrogeometries and surface treatment in early biomechanical fixation: An experimental study in dogs. *J Mech Behav Biomed Mater* 2011;4:1974–1981.
20. Marin C, Granato R, Suzuki M, Gil JN, Janal MN, Coelho PG. Histomorphologic and histomorphometric evaluation of various endosseous implant healing chamber configurations at early implantation times: A study in dogs. *Clin Oral Implants Res* 2010;21:577–583.
21. Baldassarri M, Bonfante E, Suzuki M, et al. Mechanical properties of human bone surrounding plateau root form implants retrieved after 0.3–24 years of function. *J Biomed Mater Res B Appl Biomater* 2012;100:2015–2021.
22. Coelho PG, Bonfante EA, Marin C, Granato R, Giro G, Suzuki M. A human retrieval study of plasma-sprayed hydroxyapatite-coated plateau root form implants after 2 months to 13 years in function. *J Long Term Eff Med Implants* 2010;20:335–342.
23. Coelho PG, Marin C, Granato R, Suzuki M. Histomorphologic analysis of 30 plateau root form implants retrieved after 8 to 13 years in function. A human retrieval study. *J Biomed Mater Res B Appl Biomater* 2009;91:975–979.
24. Gil LF, Suzuki M, Janal MN, et al. Progressive plateau root form dental implant osseointegration: A human retrieval study. *J Biomed Mater Res B Appl Biomater* 2015;103:1328–1332.
25. Schlee M, Pradies G, Mehmke WU, et al. Prospective, multicenter evaluation of trabecular metal-enhanced titanium dental implants placed in routine dental practices: 1-year interim report from the development period (2010 to 2011). *Clin Implant Dent Relat Res* 2015;17:1141–1153.
26. Schlee M, van der Schoor WP, van der Schoor AR. Immediate loading of trabecular metal-enhanced titanium dental implants: Interim results from an international proof-of-principle study. *Clin Implant Dent Relat Res* 2015;17(Suppl 1):e308–e320.
27. Weiss MB, Rostoker W. Development of a new endosseous dental implant. Part I: Animal studies. *J Prosthet Dent* 1981;46:646–651.
28. Coelho PG, Jimbo R, Tovar N, Bonfante EA. Osseointegration: Hierarchical designing encompassing the micrometer, micrometer, and nanometer length scales. *Dent Mater* 2015;31:37–52.
29. Ulm C, Kneissel M, Schedle A, et al. Characteristic features of trabecular bone in edentulous maxillae. *Clin Oral Implants Res* 1999;10:459–467.
30. Ulm C, Tepper G, Blahout R, Rausch-Fan X, Hienz S, Matejka M. Characteristic features of trabecular bone in edentulous mandibles. *Clin Oral Implants Res* 2009;20:594–600.
31. Froum SJ, Wallace SS, Cho SC, Elian N, Tarnow DP. Histomorphometric comparison of a biphasic bone ceramic to anorganic bovine bone for sinus augmentation: 6- to 8-month postsurgical assessment of vital bone formation. A pilot study. *Int J Periodontics Restorative Dent* 2008;28:273–281.